Multiple Forms of Short-Term Plasticity at Excitatory Synapses in Rat Medial Prefrontal Cortex

CHRIS M. HEMPEL,[1] KENICHI H. HARTMAN,[1] X.-J. WANG,[2] GINA G. TURRIGIANO,[1] AND SACHA B. NELSON[1]

Departments of [1]Biology and [2]Physics and Volen Center for Complex Systems, Brandeis University, Waltham, Massachusetts 02454

Hempel, Chris M., Kenichi H. Hartman, X.-J. Wang, Gina G. Turrigiano, and Sacha B. Nelson. Multiple forms of short-term plasticity at excitatory synapses in rat medial prefrontal cortex. *J. Neurophysiol.* 83: 3031–3041, 2000. Short-term synaptic plasticity, in particular short-term depression and facilitation, strongly influences neuronal activity in cerebral cortical circuits. We investigated short-term plasticity at excitatory synapses onto layer V pyramidal cells in the rat medial prefrontal cortex, a region whose synaptic dynamic properties have not been systematically examined. Using intracellular and extracellular recordings of synaptic responses evoked by stimulation in layers II/III in vitro, we found that short-term depression and short-term facilitation are similar to those described previously in other regions of the cortex. In additition, synapses in the prefrontal cortex prominently express augmentation, a longer lasting form of short-term synaptic enhancement. This consists of a 40–60% enhancement of synaptic transmission which lasts seconds to minutes and which can be induced by stimulus trains of moderate duration and frequency. Synapses onto layer III neurons in the primary visual cortex express substantially less augmentation, indicating that this is a synapse-specific property. Intracellular recordings from connected pairs of layer V pyramidal cells in the prefrontal cortex suggest that augmentation is a property of individual synapses that does not require activation of multiple synaptic inputs or neuromodulatory fibers. We propose that synaptic augmentation could function to enhance the ability of a neuronal circuit to sustain persistent activity after a transient stimulus. This idea is explored using a computer simulation of a simplified recurrent cortical network.

INTRODUCTION

Neurons in the mammalian cerebral cortex are interconnected into networks by synapses whose strengths can change rapidly as a function of recent activity. During repeated stimulation, excitatory and inhibitory synapses in primary visual and somatosensory cortices typically exhibit a mixture of facilitation and depression (Buhl et al. 1997; Galarreta and Hestrin 1998a; Markram and Tsodyks 1996; Reyes et al. 1998; Tamas et al. 1998; Tarczy-Hornoch et al. 1998; Thomson 1997; Thomson et al. 1993, 1996; Varela et al. 1997). Recently we, along with others, have argued that short-term plasticity at cortical synapses may strongly influence network activity (Abbott et al. 1997; Thomson and Deuchars 1994; Tsodyks and Markram 1997). In particular, depression at excitatory synapses onto pyramidal neurons and a shift in the relative balance between excitation and inhibition may tend to limit recurrent

activity and make cortical responses to sensory stimuli more transient (Chance et al. 1998; Galarreta and Hestrin 1998; Thomson and Deuchars 1994, Tsodyks and Markram 1997; Varela et al. 1999).

Unlike the transient nature of the responses of many neurons in primary visual and somatosensory cortices, neurons in many higher level association areas in the temporal (Miyashita and Chang 1988), parietal (Gnadt and Andersen 1988), and frontal lobes (Funahashi et al. 1989; Fuster 1973; Schoenbaum and Eichenbaum 1995) can exhibit persistent activity that significantly outlasts the presence of the initial stimulus. It is widely assumed that such activity reflects reverberant activation of recurrent excitatory circuits (for review see Amit 1995). If this is the case, the expression of this activity must depend critically on the steady-state balance between recurrent excitation and inhibition, which in turn must depend on the dynamic properties of synapses in these regions. Prior studies in prefrontal cortex have focused primarily on long-term synaptic change (Hirsch and Crepel 1990; Nowicky and Bindman 1993) but have also noted the existence of synaptic augmentation. Here we undertake a more systematic examination of short-term plasticity at these synapses to begin to understand regional differences in synaptic dynamics that may permit different forms of activity to be expressed in different cortical regions. Understanding synaptic dynamics in prefrontal cortex is of particular functional interest considering the implication of this area in a wide variety of integrative funcions including temporary memory, spatial orientation, sequential organization of behaviors, sexual and social behaviors, and behavioral flexibility in the rat (for review see Kolb 1990) and working memory, attention, reasoning, and planning in primates (for review see Grafman et al. 1995, Uylings et al. 1990).

Using a combination of field potential and single and dual whole cell recording, we find that depression and rapid facilitation of excitatory input to layer V neurons are similar to that previously observed in layer II/III of primary visual cortex and by others in layer V of somatosensory cortex. In addition, these experiments revealed prominent short-term synaptic enhancement lasting seconds to minutes. Paired recordings between layer V neurons revealed that the augmentation could be evoked at unitary connections within the prefrontal cortex and therefore did not require activation of afferents from other regions, release of extrinsic neuromodulators, or activation of a large network of neurons. These experiments suggest that brief periods of synaptic activity may be able to transiently shift a set of interconnected cortical neurons into a state in

which recurrent excitation is sufficiently strong to support persistent activity. Incorporation of the observed synaptic dynamics into a computer simulation of a simplified recurrent cortical network supports this idea by showing that augmentation can help to sustain activity in response to a transient input.

METHODS

Tissue preparation

Brain slices were obtained from Long Evans rats aged 15–19 days postnatal (intracellular recordings) or 19–25 days (field-potential recordings). Rats of different ages were used because robust field potentials could be more reliably evoked in older animals whereas patch-clamp recordings were easier to obtain in slices from younger animals. Animals were deeply anesthetized with a 1:1 mixture of ketamine and acepromazine, decapitated, and their brains rapidly removed and placed in cold ($<4°C$) artificial cereberospinal fluid (ACSF). Coronal slices (400–500 μm thick) were cut on a vibratome at the level of the frontal cortex or visual cortex and placed in a room-temperature incubation chamber. All prefrontal cortex recordings were made in medial frontal cortex, a region that has alternately been referred to as anterior cingulate or prelimbic cortex. The anatomic locations of these recordings were assessed with reference to Paxinos and Watson (1986), using shape of the subcortical white matter as the primary landmark. The anterior/posterior position of slices matched plates 9, 10, or 11 of the atlas. Dorsal ventral position ranged from 1.5 to 3.5 mm ventral to the dorsal pial surface. These coordinates placed the recording sites primarily in areas designated Cg_1 and Cg_3, with some sites near the border of Cg_2.

Electrophysiological recordings

Slices were transferred to a recording chamber and perfused at 1–2 ml/min with oxygenated ACSF (28–32°C). At least 30 min were allowed for equilibration. During extracellular field-potential recordings slices were viewed at low magnification. Stimulation and recording pipettes, both with tip diameters 30–50 μm, were filled with ACSF and lowered 25–75 μm below the surface of the slice. Stimulus isolation units delivered biphasic stimulus pulses (20–200 μA, 100 μs/phase with 100-μs interval). Field potentials were filtered with a band-pass of 1–1000 Hz and amplified with a differential amplifier (A & M Instruments). Visually guided whole cell patch-clamp recordings were made using an Olympus BX50WI microscope equipped with infrared differential interference contrast optics. Recording pipettes had a resistance of 3–5 Mohms when filled with recording solution. Voltage-clamp recordings were made using an Axopatch 200B patch-clamp amplifier (Axon Instruments), low-pass filtered at 2 kHz. Whole cell recordings were rejected if they did not meet the following criteria: resting potential more negative than −50 mV and input resistance (measured at −70 mV with −5 mV pulses) > 100 Mohm. Intracellularly recorded synaptic currents were evoked using smaller stimulating pipettes ($\sim$1–2 μm diam) and correspondingly smaller stimulating currents (2–20 μA) than those used to evoke synaptic field potentials. All intracellular and extracellular recordings in prefrontal cortex were made in layer V ($\sim$600–800 μm from pial surface); extracellular recordings from visual cortex were made in layer II/III (300–400 μm from pial surface). Extracellular stimulation sites were in layer II/III (prefrontal cortex; 300–500 μm from pial surface) or layer IV (visual cortex; 400–600 μm from pial surface) and were always aligned with recording sites along the axis perpendicular to the pial surface.

Solutions

ACSF contained (in mM) 126 NaCl, 3 KCl, 1.25 NaH_2PO_4, 10 dextrose, 20 $NaHCO_3$, 2 $MgSO_4$, and 2.0 $CaCl_2$. Osmolarity was 305–310 mOsm and pH 7.4 when equilibrated with 95% O_2-5% CO_2. Whole cell patch pipettes were filled with a solution with pH between 7.2 and 7.4 and containing (in mM) 130 potassium methylsulfonate, 10 KCl, 2 $MgSO_4$, 10 HEPES, 0.1 or 0.5 EGTA, and 3 ATP (potassium salt). APV (+/−) was supplied by Research Biochemicals International.

Data analysis

All recordings were digitized at 5–10 kHz, stored, and analyzed using IGOR software (Wavemetrics, Lake Oswego, OR). Synaptic efficacy was determined from field postsynaptic potentials (fPSPs) using peak amplitude measurements. Evoked field potentials consisted of two, usually well-separated components (Fig. 2A): an early, biphasic component often overlapping with the stimulus artifact followed by a negative component of longer duration. Pharmacologic manipulations (Varela et al. 1997) identified the early component as the field action potential (fAP) resulting from synchronous action potentials in those neurons directly activated by the stimulus, and the second component as the fPSP, in agreement with Morris et al. (1999). The location of the fPSP peak was found algorithmically within a user-specified window and response amplitude was quantified as the mean amplitude of a 0.2-ms segment centered on the peak location. The duration and location of the user-specified window varied between recording sites but was confined to a latency of <5 ms. In cases where later, presumably polysynaptically activated synaptic potentials overlapped with the initial peak, the user-specified window was placed before the point of inflection separating the two components. Synaptic efficacy was determined from intracellular postsynaptic currents (PSCs) using two measurements: peak PSC amplitude and early PSC slope. Peak amplitude was calculated as the mean amplitude of the evoked PSC waveform over a 1.0-ms window centered on the peak. Early slope was calculated using linear regression applied to a 1-ms segment of the PSC waveform starting 0.1–0.9 ms after onset. fPSP amplitude was monitored at a low frequency of 0.1 Hz to avoid short-term synaptic depression. For PSCs whose response amplitudes were substantially more variable, a higher monitoring frequency of 0.5 Hz was necessary to provide a better estimate of synaptic efficacy.

Computer simulations

To explore the potential functional roles of short-term synaptic enhancement, we simulated a network model of leaky integrate-and-fire neurons that are densely connected in an all-to-all fashion. These simulations were based on the model of persistent activity developed in (Wang 1999a) with the addition of short-term synaptic enhancement. Each model neuron obeys the following equation

$$C_m \frac{dV_m}{dt} = -I_L - I_{syn} + I_{ext} \qquad (1)$$

where C_m is the capacitance and the leak current $I_L = g_L (V_m - V_L)$. A spike is discharged each time V_m is driven to reach a firing voltage threshold V_{th}. V_m is reset to V_{reset} and stays there for an absolute refractory period τ_{ref}. $C_m = 0.5$ nF and $g_L = 25$ nS (so that time constant $\tau_m = C_m/g_L = 20$ ms); $V_L = -70$, $V_{th} = -52$, and $V_{reset} = -59$ (in mV); and $\tau_{ref} = 2$ ms. $I_{syn} = I_{AMPA} + I_{NMDA}$ is the total recurrent synaptic current from other pyramidal cells. I_{ext} represents the afferent input to the network, $I_{ext} = g_{ext}s_{ext} (V_m - E_{syn})$, where $g_{ext} = 0.0015$ μS. I_{ext} is assumed to be mediated by AMPA receptors and the conductance change is a convolution of a Poisson input train at rate λ_{input} with a unitary conductance that decays exponentially with a time constant of 2 ms.

Recurrent excitatory postsynaptic currents (EPSCs) consist of two components, I_{AMPA} and I_{NMDA}. The AMPA receptor-mediated current $I_{AMPA} = g_{AMPA}s(V_m - E_{syn})$, with $E_{syn} = 0$ mV. To capture the rise and decay kinetics of synaptic currents and their saturation, the

gating variable s (the fraction of open channels) is described by two first-order kinetics

$$\frac{dx}{dt} = \alpha_x \sum_j \delta(t - t_j) - x/\tau_x; \quad \frac{ds}{dt} = \alpha_s x(1 - s) - s/\tau_s \quad (2)$$

where the sum is over presynaptic spike times. For the AMPA receptor channels, $\tau_x = 0.05$ ms and $\tau_s = 2$ ms (time-to-peak is 0.2 ms); $\alpha_x = 1$ (dimensionless) and $\alpha_s = 1$ (in ms^{-1}). The NMDA receptor-mediated current $I_{NMDA} = g_{NMDA}s(V_m - V_E)/(1 + [Mg^{2+}] \exp(-0.062V_m)/3.57)$ (Jahr and Stevens 1990), with a voltage-dependence controlled by the extracellular magnesium concentration $[Mg^{2+}] = 1.0$ mM. The gating variable s obeys the same types of equations (*Eq. 2*) but with $\tau_x = 2$ ms, $\tau_s = 80$ ms (time-to-peak is 8 ms), $\alpha_x = 1$ (dimensionless), and $\alpha_s = 0.3$ (in ms^{-1}). The ratio of the NMDA- versus AMPA-receptor mediated EPSC is 2% in peak current ($g_{AMPA} = 0.03$, $g_{NMDA} = 0.0012$) and 75% in terms of the charge entry (resting potential of -70 mV).

To implement short-term synaptic plasticity, the parameter α_x is multiplied by DF, where D and F describe depression and facilitation, respectively. Short-term depression is assumed to be caused by transmitter vesicle depletion at presynaptic terminals (Galarreta and Hestrin 1998b; Stevens and Wang 1995; Varela et al. 1997). The depression factor D is initially 1; it is reduced by a factor $(1 - p_vF)$ for each spike and recovers with time constant τ_D in the absence of stimuli (Abbott et al. 1997; Markram and Tsodyks 1996). The parameter p_v is the release probability per vesicle in a simple model of short-term depression by vesicle depletion (Wang 1999b). We used $\tau_D = 300$ ms and $p_v = 0.60$.

The facilitation factor F obeys the following dynamical equation (Bertram et al. 1996; Wang 1999b)

$$\frac{dF}{dt} = \alpha_F[Ca^{2+}](1 - F) - F/\tau_F$$

Two modifications were made to the model of Bertram et al. (1996). First, the model was reformulated for spikes as point events in time. Second, and more importantly, contributions from residual presynaptic calcium were included (see Zucker 1993). Thus the intracellular calcium $[Ca^{2+}]$ consists of two components

$$[Ca^{2+}](t) = [Ca^{2+}]_{peak} \sum_j \delta(t - t_j) + [Ca^{2+}]_{res}(t).$$

$[Ca^{2+}]_{peak} = 250$ (in μM $\cdot$ ms) represents the time-integral of the brief spike-triggered $[Ca^{2+}]$ transient, which is >100 μM for a few milliseconds per spike (Llinás et al. 1981; Zucker 1993). At the end of the rapid transient pulse there is a residual $[Ca^{2+}]_{res}$ with a much smaller amplitude and slower decay. $[Ca^{2+}]_{res}$ is incremented by 0.1 μM/spike and decays with a time constant of 2 s (Regehr et al. 1994). We used $\alpha_F = 0.0035$ [in $(\mu$M $\cdot$ ms)$^{-1}$]; $\tau_F = 7000$ (in ms). The value of τ_F was chosen to match the fast time constant of augmentation observed experimentally (see RESULTS).

In some simulations we blocked synaptic augmentation. In this case, the parameter α_x is multiplied by the initial value of F so that the synaptic conductance change $s(t)$ produced by a single spike remains the same. In addition, the amount of short-term depression was preserved by setting the initial release probability to 0.60.

Statistics

Sample means are reported $\pm$ SE throughout unless otherwise indicated. Statistically significant differences between population means are assessed using Student's t-tests with a confidence level of $P < 0.05$. Student's t-tests were two-tailed unless otherwise indicated.

RESULTS

To characterize synaptic dynamics in prefrontal cortex we recorded intracellularly from visually identified layer V pyra-midal cells. Stimuli delivered to layer III were adjusted in intensity to produce predominantly monosynaptic, excitatory synaptic currents between 30 and 200 pA in amplitude (mean 102 pA, $n = 7$; sample traces in Fig. 1A). A synaptic current was scored as monosynaptic if its onset latency (time to 5% of peak response) was constant at <4.0 ms (mean 2.6 ms) and the
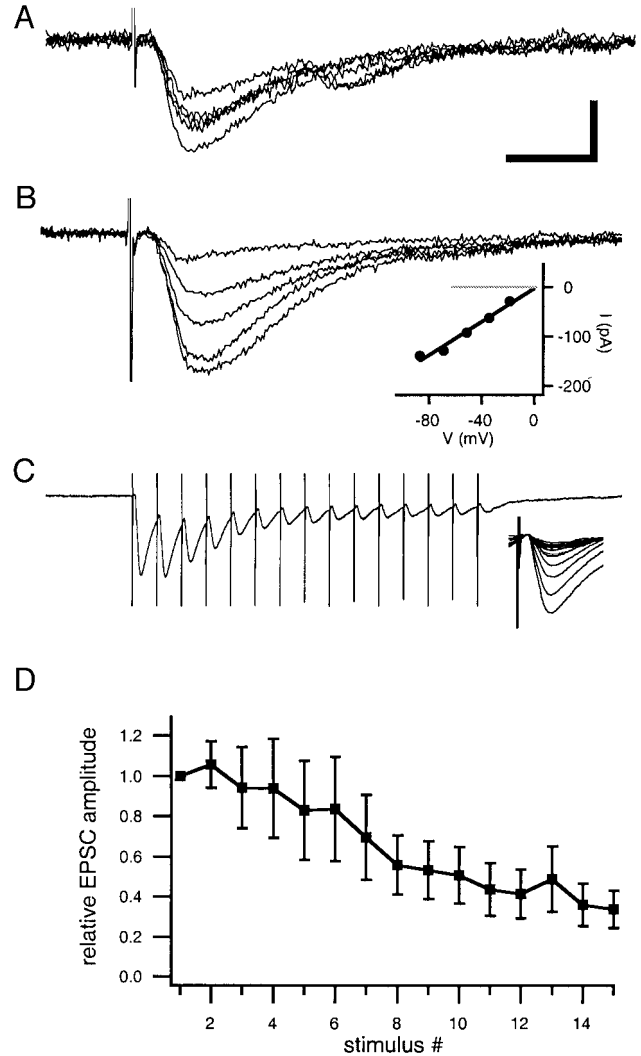

FIG. 1. Short-term depression of excitatory postsynaptic currents (EPSCs) recorded in prefrontal cortex layer V. *A–C*: voltage-clamp traces are from different neurons. Scale bar in *A* represents 5 ms, 50 pA for *A* and *B*; 120 pA, 75 ms (*inset,* 20 ms) for *C*. *A*: individual synaptic currents recorded from a visually identified layer V pyramidal neuron. Membrane potential was clamped at -70 mV and EPSCs were evoked by layer III stimulation at a frequency of 0.5 Hz. Five successive, individual responses are displayed demonstrating a constant latency of <2 ms and variation in amplitude. *B*: reversal potential of evoked synaptic currents in a layer V pyramidal cell. Intracellular postsynaptic currents (PSCs) were evoked during membrane potential steps to -87, -69, -51, -34, and -18 mV (corrected for series resistance error). Each trace is a leak-subtracted average of 5 trials. *Inset*: peak amplitudes of these evoked PSCs plotted against membrane potential. Linear fit shows an extrapolated reversal potential of $+1$ mV. *C*: short-term depression of EPSCs. EPSC amplitude is attenuated during a 50-Hz train of extracellular stimulation. Traces are averaged over 30 repetitions. *Inset*: individual, averaged EPSCs extracted superimposed. *D*: mean short-term depression across experiments. Dots represent mean peak EPSC amplitudes during 50-Hz trains ($n = 7$ neurons) normalized to the amplitude of the first PSC in the train. To compensate for summation of PSCs within the train, amplitudes of each PSC were calculated by subtracting from the peak amplitude a baseline value reflecting extrapolated decay of previous EPSCs.

current rose to 95% of its peak value in <8.0 ms (mean 5.3 ms).

To quantify the efficacy of synaptic transmission we measure peak PSC amplitudes. To obtain a measure free from polysynaptic contamination, we also measured early PSC slope (see METHODS); however, these measurements were typically much noisier. Linear regression analysis on pooled and normalized sets of recordings in which EPSCs were varied over a range of ~50% by augmenting stimuli showed that the two measures correlated well ($R = 0.9$; $P = 2 \times 10^{-20}$). This justifies the use of peak PSC amplitude as an index of monosynaptic transmission.

To establish the reversal potential of these monosynaptic responses, we performed a set of experiments under conditions identical to those used throughout the paper but with action potentials blocked by intracellular QX-314 (10 mM). Because QX-314 had complicated effects on synaptic transmission and plasticity it was not used routinely. These experiments showed that the early portion of the response (<8 ms relative to stimulus onset) reversed at -6.8 ± 4.9 (SE) mV ($n = 5$; Fig. 1B). These results indicate that the monosynaptic response reflects activation of primarily excitatory glutamatergic synapses. In some recordings, later portions of the response (>8 ms relative to stimulus onset) had more negative reversal potentials suggesting a contribution of a polysynaptically activated GABAergic, inhibitory current. This did not contaminate the peak amplitude measurements which were made only on the early component of the complex PSC.

Evoked EPSCs exhibited strong short-term depression during high-frequency stimulus trains (Fig. 1, B–D). Over the course of a 50-Hz train for example, EPSC amplitudes decreased to $40 \pm 6\%$ of their initial value ($n = 7$, Fig. 1D). In two of seven cells tested, however, short-term facilitation dominated the early part of the train, with EPSCs almost doubling in amplitude before dropping below baseline levels toward the end of the train. This between-cell variability in facilitation is reflected in Fig. 1D as an increase in the size of SE bars from pulse numbers 3–8 and as a deviation from the smooth, exponential decay profile expected from pure synaptic depression.

To further characterize short-term synaptic plasticity in the prefrontal cortex we measured synaptic field potentials (fPSPs). The long-term stability and high signal to noise ratio of fPSP recordings make them a useful adjunct to intracellular recording. In particular, they enable a systematic, parametric analysis of regional synaptic properties. Therefore we used fPSP measurements to determine the dependence of short-term facilitation and short-term depression on the frequency and duration of the conditioning tetanus. Amplitudes of fPSPs evoked by stimulation in layer III and recorded in layer V were constant over extended periods of low frequency (0.1 Hz) stimulation. As with intracellularly recorded EPSCs, however, higher frequency (1–50 Hz) stimulation produced strongly depressing fPSPs (Fig. 2, A and B). This short-term depression was most pronounced at the end of a train where field-potential amplitudes had reached a nearly steady state. To quantify this process we calculated the "steady-state ratio," the ratio of the last response to the first response. This quantity varied as a function of the frequency of stimuli within the train (Fig. 2C). However, fPSP amplitude did not decay to steady-state levels in a smooth fashion (Fig. 2B). Rather, as with EPSCs, a second, facilitatory process appeared to exert an influence on fPSP
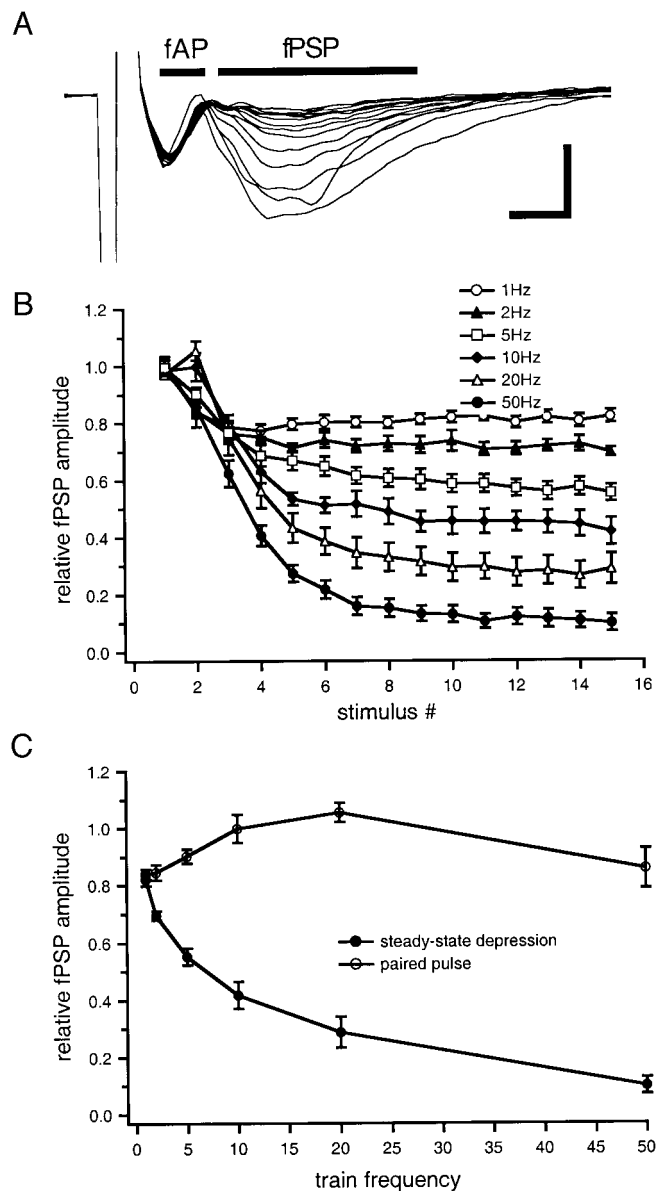

FIG. 2. Frequency dependence of short-term synaptic depression in prefrontal cortex measured with synaptic field potentials (fPSPs). A: short-term depression of evoked fPSPs recorded from layer V of prefrontal cortex during stimulation of layer III. Individual responses to the 15 stimuli within a 50-Hz train are superimposed. The 2 components of response are indicated [field action potential (fAP) and fPSP; see METHODS]. Scale bar represents 2 ms, 200 μV. B: frequency dependence of short-term depression. Individual points represent mean fPSP amplitudes during trains of 15 stimuli delivered at indicated frequencies. Traces are normalized to amplitude of the first fPSP in the train. Each frequency was tested in 5 separate experiments. C: data from 2nd stimulus (white circles) and 15th stimulus (black circles) in B replotted as a function of stimulus frequency. Plotting along frequency coordinate emphasizes absence of correlation between paired-pulse amplitude and steady-state amplitude.

amplitude, most prominently at the beginning of the train. To quantify the contribution of this process we calculated the "paired-pulse ratio" as the amplitude of the second response divided by that of the first. This index also varied as a function of the frequency of stimuli within the train (Fig. 2C), albeit with a profile different from that of the steady-state ratio. These results are consistent with the presence of two competing short-term plasticity phenomena influencing synaptic transmis-

sion during a high-frequency train: short-term facilitation and short-term depression. Because their timecourses overlap, deconvolution of the two processes would require either a pharmacologic separation or a more detailed quantitative analysis (Varela et al. 1997).

The short-term changes in fPSP amplitude were accompanied by only small changes in the amplitude of the presynaptic population action potential (fAP), ruling out the possibility that these changes could be attributed primarily to changes in presynaptic excitability. During 50-Hz trains, fAP amplitude of the second and last responses changed relative to the initial response on average by $-7 \pm 3\%$ and $+2 \pm 7\%$ (mean $\pm$ SE, $n = 4$ slices). Similarly, during augmentation (see next paragraph) fAP amplitude was changed by $-5 \pm 3\%$ relative to baseline (mean $\pm$ SE, $n = 4$). Thus changes in fPSP amplitude reflected primarily a change in efficacy of synaptic transmission.

In addition to short-term facilitation and depression, occurring on a timescale of tens to hundreds of milliseconds, we observed a posttetanic enhancement of synaptic transmission occurring on the timescale of seconds to tens of seconds (Fig. 3). Again, this was observed using both intracellular and extracellular recordings. EPSCs evoked immediately after a 50-Hz, 15-pulse tetanus were $55 \pm 10\%$ larger than those sampled before the tetanus (Fig. 3C; $n = 7$). The decay of this enhancement could be best fit with a sum of two exponentials with fast and slow decay time constants of 7 and 71 s, respectively. Short-term enhancement on these time scales is classically called augmentation and posttetanic potentiation for the short and long phases, respectively (Zengel and Magleby 1982). However, because we had no further evidence of multiple processes we will refer to all phases of this enhancement collectively as "augmentation."

In general, fPSPs corroborated the observations made with intracellular recordings (Fig. 3D). A $41 \pm 10\%$ ($n = 5$) augmentation was produced in layer V of the prefrontal cortex. Curiously, the apparent decay rate of augmentation depended on the assay, particularly the fast component of the decay. When measured using field-potential recordings, the timecourse of decay could be best fit with two exponentials with fast and slow decay constants of 19 and 74 s (fits performed on pooled data shown in Fig. 3D). Analogous fits to the whole cell data (Fig. 3C) yielded a similar slow decay constant of 71 s but a shorter fast decay constant of 7 s. This could reflect differences in the population of synapses stimulated, differences in the sampling frequency used (0.5 Hz for intracellular recordings vs. 0.1 Hz for the extracellular recordings), or differences in the age of animals used in the two recording configurations (see METHODS).

Augmentation was robust and reliably reproducible in layer V of the prefrontal cortex. In contrast, EPSCs in visual cortical pyramidal neurons exhibit little or no augmentation (Varela et al. 1997). We confirmed this result with a series of experiments carried out in visual cortex slices using the same recording configuration used by Varela et al. (1997), namely fPSPs elicited by extracellular stimulation in layer IV and recorded in layer III. A $10 \pm 1.5\%$ increase in fPSP amplitude ($n = 5$) was produced by 50-Hz, 15-pulse tetanii compared with a $41 \pm 10\%$ increase ($n = 5$) under identical conditions in prefrontal cortex. The difference between prefrontal and primary visual cortices was significant ($P = 0.0002$). We did not systematically test other pathways in either cortical area and therefore
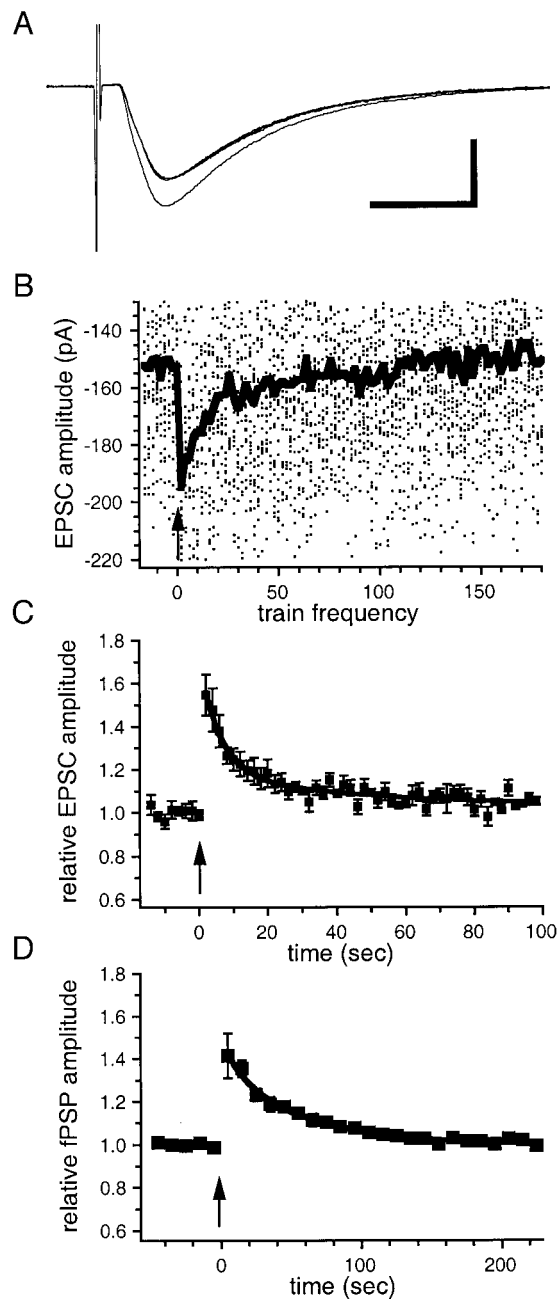

FIG. 3. Different magnitudes of augmentation between prefrontal cortex layer V and primary visual cortex layer III. A: augmentation of EPSCs recorded from a layer V pyramidal cell in prefrontal cortex. Superimposed records, each an average of 30 repetitions, taken 30, 20, and 10 s before and 20 s after a 50-Hz, 15-stimulus tetanus is applied. Scale bar represents 10 ms, 100 pA. B: peak EPSC amplitudes from cell shown in A. EPSCs were sampled at 0.5 Hz before and after tetanus (arrow). Mean across 30 repetitions (solid line) is plotted along with amplitudes for each individual repetition (dots). C: augmentation of EPSCs in prefrontal cortex. Points represent mean EPSC amplitudes from layer V pyramidal neurons in prefrontal cortex ($n = 7$) subjected to the protocol described in B. Traces from individual experiments were normalized to their own pretetanus baseline before averaging, which resulted in a scale inversion. Best-fit sum of 2 exponentials is shown (solid line). D: augmentation of fPSPs in prefrontal cortex. Points represent mean fPSC amplitudes recorded in layer V of prefrontal cortex ($n = 5$). Traces from individual experiments were normalized to their own pretetanus baseline before averaging. Best-fit sum of 2 exponentials is shown (solid line).

cannot assess whether this difference in synaptic properties reflects primarily differences within or between cortical areas.
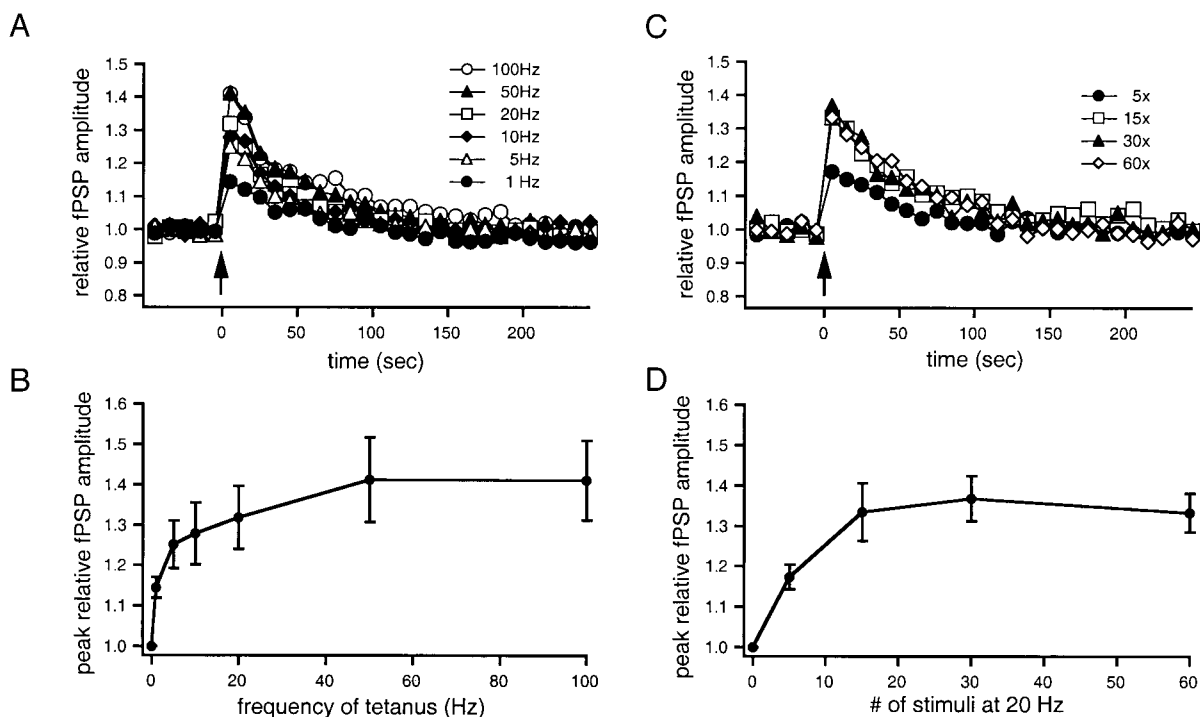
FIG. 4. Dependence of synaptic augmentation on tetanus frequency and length. *A*: fPSP amplitudes sampled at 0.1 Hz in layer V of prefrontal cortex before and after tetanii of varying frequency and fixed length (15 stimuli). Each trace represents the baseline-normalized average of 5 experiments. Error bars have been omitted to minimize clutter. *B*: peak augmentation amplitude as a function of stimulus frequency. Data points represent the first posttetanic response shown in *A* plotted against stimulus frequency. *C*: fPSP amplitudes sampled at 0.1 Hz in layer V of prefrontal cortex before and after tetanii varying in length from 5 to 60 pulses at a fixed frequency of 20 Hz. Each trace represents the baseline-normalized average of 5 experiments. *D*: peak fPSP amplitude as a function of number of stimuli in a 20-Hz train. Data points represent the first posttetanic response shown in *C* plotted against number of stimuli.

We used field-potential recordings to quantify the dependence of augmentation in prefrontal cortex on the frequency and duration of the conditioning tetanus (Fig. 4). For trains of 15 stimuli, frequencies as low as 1–5 Hz produced augmentation, which appeared to saturate at frequencies of 50–100 Hz (Fig. 4, *A* and *B*). For trains at a fixed frequency of 20 Hz, as few as five stimuli produced augmentation, saturating with 15–30 stimuli (Fig. 4, *C* and *D*). These values are well within the physiological activity range of cortical neurons.

We also used field-potential recordings to examine the role of the NMDA receptor in the induction or expression of augmentation. Application of the NMDA receptor antagonist APV (50 μM) did not prevent augmentation; 15-stimulus, 50-Hz trains enhanced fPSPs by 56 $\pm$ 2% ($n = 3$; not shown). Thus NMDA-receptor activation does not appear to be required for augmentation in the prefrontal cortex in contrast to some forms of short-term enhancement that have been demonstated in the hippocampus (Malenka 1991) and the somatosensory cortex (Castro-Alamancos and Connors 1996).

The fPSPs and EPSCs described thus far were evoked by extracellular stimulation. This does not permit the identification of activated presynaptic neurons with respect to their precise location and cell type. In addition, extracellular stimulation can excite neuromodulatory fibers and/or generate polysynaptic network activity, both of which could account for the induction of augmentation. To address these problems and directly test if a train of presynaptic action potentials in a single identified presynaptic neuron could produce synaptic augmentation, we recorded intracellularly from synaptically connected pairs of adjacent, visually identified layer V pyramidal neurons in the prefrontal cortex (Fig. 5*A*). Approximately one of five tested pairs showed a one-way synaptic connection, which is a connection probability similar to that found for these pairs in somatosensory cortex (Markram et al. 1997). Six pairs were held long enough to administer several repetitions of an augmentation-inducing protocol. Pooled data from these pairs revealed short-term depression (average of last 4 EPSCs was 33 $\pm$ 9% of initial EPSC amplitude; Fig. 5*C*) and augmentation (first posttetanic pulse enhanced 56 $\pm$ 12% over control; Fig. 5*D*). Although the variability in EPSC amplitude was relatively large, both effects were statistically significant. In the case of short-term depression the first EPSC in the train was compared with the last five in an unpaired *t*-test ($P = 0.003$). For augmentation, the last five pretetanic EPSCs were compared with those of the first posttetanic EPSC in an unpaired *t*-test ($P = 0.002$). Variability in the paired-recording data precluded accurate measurement of the augmentation decay timecourse.

To explore the possible function of synaptic augmentation in the prefrontal cortex, we performed computer simulations of a simple network model for persistent activity. The model consists of 100 completely interconnected pyramidal neurons. In addition to recurrent input from other neurons in the network, each neuron receives random spontaneous input representing ongoing drive from extrinsic afferents. The details of the simulation are based on well-described properties of cortical networks such as the frequency-current relation of pyramidal neurons, time courses of the AMPA-receptor and NMDA-receptor mediated synaptic currents, recurrent excitation, and
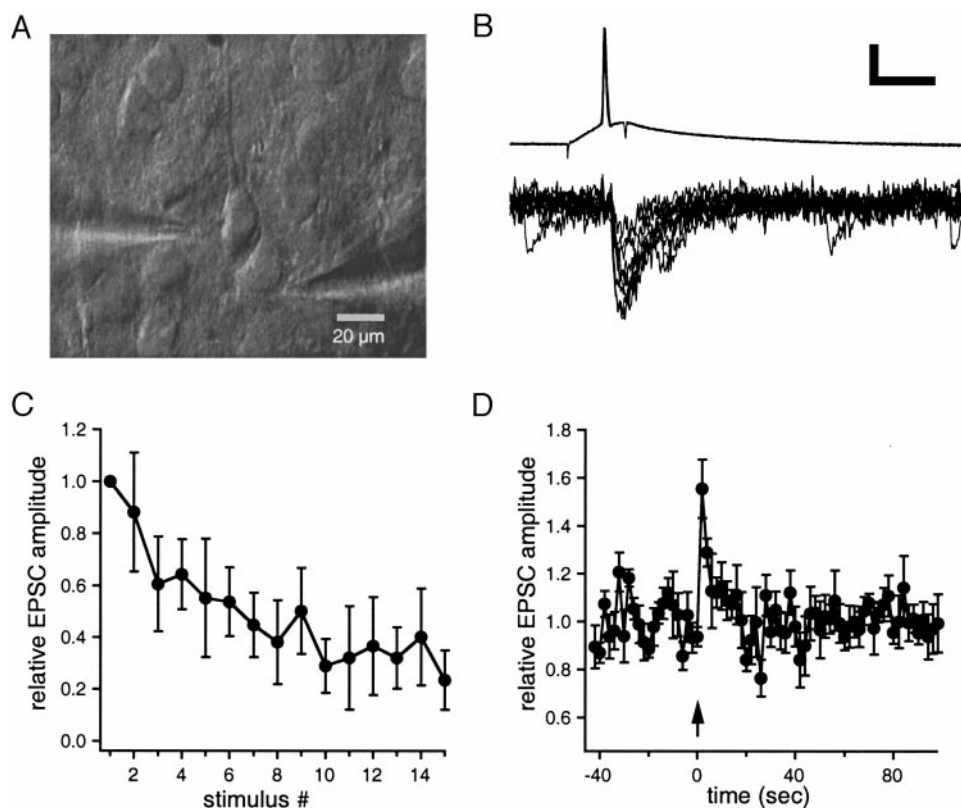
FIG. 5. Synaptic augmentation and short-term depression of EPSCs at synapses between layer V pyramidal cells in prefrontal cortex. *A*: infrared differential interference contrast image of a pair of layer V pyramidal neurons in a prefrontal cortex slice. Recording pipettes are attached to each cell. *B*: presynaptic current clamp (*top*) and postsynaptic voltage clamp recordings from a synaptically connected pair of layer V pyramidal cells. Each panel shows 10 superimposed individual sweeps. Scale bar represents 30 mV/10 pA, 10 ms. *C*: short-term depression at synapses between layer V pyramidal cells. Data points represent mean EPSC amplitudes from 6 connected pairs plotted as a function of stimulus number during a 50-Hz, 15-stimulus train of presynaptic action potentials. EPSC amplitudes were normalized to the first response for each pair before averaging. *D*: augmentation at synapses between layer V pyramidal cells. Data points represent mean EPSC amplitudes sampled at 0.5 Hz from 6 connected pairs before and after a 50-Hz, 15-stimulus train of presynaptic action potentials. EPSC amplitudes were normalized to a 40-s baseline period for each pair.

synaptic depression (see METHODS for details). We were interested in whether adding augmentation to such a network would endow it with the capability for persistent activity that outlasts a transient stimulus. The basic features of synaptic transmission within the model are illustrated in Fig. 6. A short current pulse delivered into a presynaptic cell produces a single presynaptic spike and an EPSP of 0.3 mV in a postsynaptic cell. A longer current pulse produces a train of action potentials (22 spikes at 50 Hz) in the presynaptic cell during which EPSPs first facilitate and then depress. A final short current pulse again produces a single action potential which elicits an enhanced EPSP (60% increase after a time interval of 3 s). Note that as a result of the slow decay of the residual presynaptic $[Ca^{2+}]$, the facilitation factor F is reduced only by a small amount between the tetanus and the second test stimulation.

Figure 7 shows a simulation of the recurrently connected network in the presence of afferent input that causes the membrane potential of all neurons to fluctuate near their firing threshold. A transient increase of the rate of afferent input induced neuronal spike discharges. In the absence of short-term synaptic enhancement (Fig. 7*A*), the recurrent connections are weak and the activity dies out at the end of stimulation with the chosen set of model parameters. With short-term synaptic enhancement included in the model (Fig. 7*B*), recurrent synapses are temporarily strengthened during the neural response to the stimulus. As a result, network activity, sustained by sufficiently strong, recurrent synaptic excitation, now outlasts the transient input. The persistent network activity is terminated by a step decrease in the rate of afferent input.

Because of short-term depression, the neuronal firing rate decreases greatly during the transient stimulus (Fig. 7*A*). This effect has been observed in recordings from prefrontal cortical

neurons in behaving animals (Funahashi et al. 1989; Romo et al. 1999). Moreover, persistent activity is sustained in the network at relatively low firing rates (~50 Hz), which are within the observed range of rates for prefrontal cortical neurons in behaving animals (Funahashi et al. 1989; Rainer et al. 1998). This is worth noting because in a strongly recurrent excitatory network, rate control is needed so that neurons are not driven to saturation (firing at 100s of Hz) caused by the powerful positive feedback. This is accomplished in the present model by short-term depression of the recurrent synapses. If short-term depression is not included in the simulation, model neurons fire at >400 Hz in the persistent state (not shown). Although short-term depression is important for controlling the rate of persistent activity in the model, it is not used to terminate this activity. The actual biological mechanisms by which persistent activity might be terminated are not understood and are not addressed in these simulations.

DISCUSSION

The results presented here demonstrate that excitatory synapses in rat medial prefrontal cortex exhibit short-term depression and short-term facilitation that are similar to those observed in primary visual cortex (Varela et al. 1997). These experiments also revealed, however, that short bursts of action potentials at moderate frequency produce synaptic augmentation of up to 50%, lasting seconds to minutes. This property was observed using field-potential recordings, intracellular recordings with extracellular stimulation, and intracellular recordings from synaptically connected pairs of layer V pyramidal cells, the latter indicating that augmentation is a property of intrinsic synapses. The capacity for augmentation is expressed

differentially in the cortex, because it was largely absent in at least one class of synapse in the visual cortex, namely excitatory synapses onto layer II/III pyramidal cells.

Rapid depression and facilitation

During a 50-Hz, 15-stimulus train, synaptic currents in layer V pyramidal neurons in prefrontal cortex are reduced to between 20 and 40% of their initial amplitude. Both the magnitude of this depression and its frequency dependence were similar to those observed at synapses onto layer III pyramidal cells in primary visual cortex using the same techniques (see Fig. 1*B* in Abbott et al. 1997; see also Varela et al. 1997, 1999). The fact that short-term synaptic depression has been observed in all cortical areas that have been examined (Buhl et al. 1997; Galarreta and Hestrin 1998a; Markram and Tsodyks 1996; Reyes et al. 1998; Tamas et al. 1998; Tarczy-Hornoch et al. 1998; Thomson 1997; Thomson et al. 1993, 1996; Varela et al. 1997) suggests that it is a general property of cortical circuitry. This may reflect a general need in cortical circuits for synapse-specific gain control, which short-term depression can provide (Abbott et al. 1997). The ubiquity of short-term depression may however, be a particular feature of the developing cortex and may give way to more heterogeneous dynamic properties of synapses in the adult (Angulo et al. 1999; Reyes et al. 1998; Y. Zhuo and S. B. Nelson, unpublished observations).

Synaptic responses in prefrontal cortex typically exhibited less paired-pulse depression (i.e., between the first and second stimulus in the train) than that expected on the basis of steady
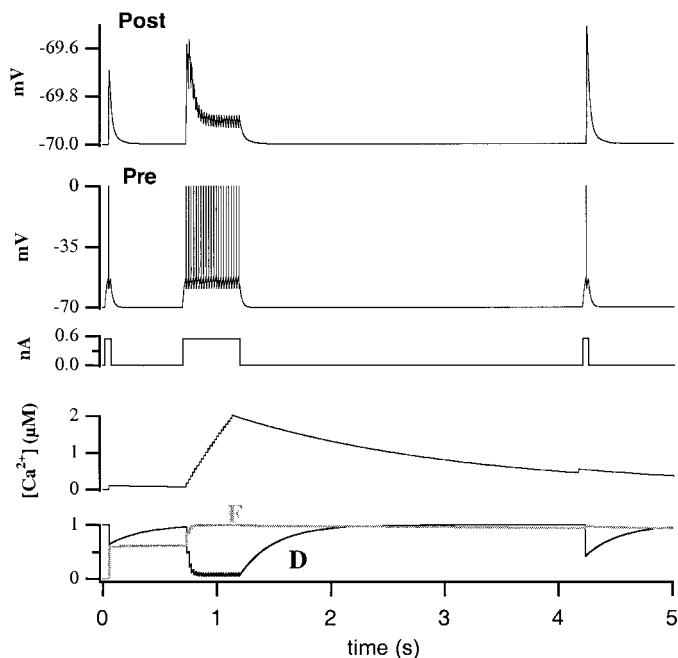

FIG. 6. Computer simulation of a 2-neuron pair coupled by synapses incorporating short-term depression and augmentation. A pre- and postsynaptic pair of model neurons is shown to illustrate the plastic properties of simulated synapse. *Top–bottom*: membrane potentials of postsynaptic and presynaptic cells, input current to presynaptic cell, residual calcium in presynaptic terminals $[Ca^{2+}]_{res}$, depression factor *D*, and facilitation factor *F* (see METHODS). Note initial facilitation, followed by depression, of EPSPs during tetanus. A test pulse 3 s after the tetanus generated a response 60% larger than that of a pretetanic test pulse. No additional synaptic input was present in this simulation.
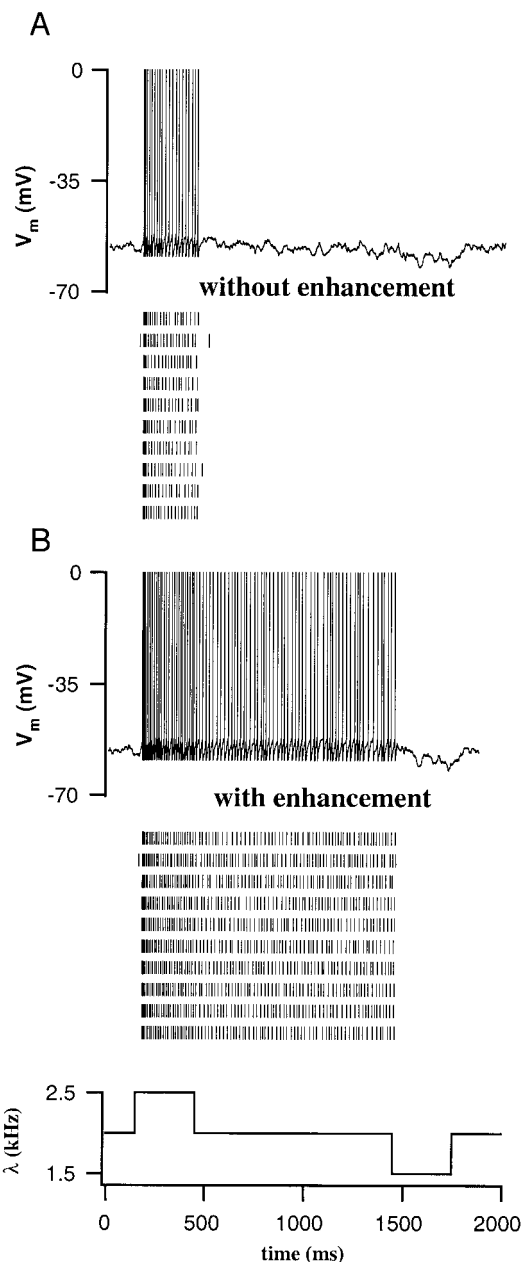

FIG. 7. Transient input produces persistent activity in model network endowed with short-term synaptic enhancement. *A*: model parameters were chosen such that without short-term enhancement, the recurrent synapses were not strong enough to sustain a persistent activity through reverberating excitation in the network. Brief increase of external drive (λ_{input}, *bottom*) produces transient neuronal responses which show a decreasing firing rate caused by short-term depression of recurrent synapses. *Trace*: activity of a single cell and rastergram shows firing patterns of 10 representative cells in the 100-neuron network. *B*: with short-term synaptic enhancement included in the model, the same brief increase in external input generates network activity that now outlasts the stimulus and is terminated later by a brief decrease in the external drive.

state responses (Fig. 2, *B* and *C*). This may reflect simultaneous facilitation which can be readily demonstrated at cortical synapses under conditions of reduced transmitter release (Varela et al. 1997). Short-term depression and short-term facilitation are known to be coexpressed in the same synaptic pathways at some central synapses (Stevens and Wang 1995), however their relative proportions can vary between different output

synapses of the same neuron (Markram et al. 1998; Reyes et al. 1998). We have not attempted to separate the influence of facilitation and depression at synapses in prefrontal cortex, but the fact that the two forms of plasticity can overlap temporally means that paired pulse protocols may be of limited value for predicting steady state synaptic responses.

Synaptic augmentation

Some of the earliest studies concerning synaptic plasticity, such as those carried out on the vertebrate neuromuscular junction (Feng 1941) and spinal cord (Kuno 1964), were concerned with synaptic enhancement lasting seconds to minutes. These forms of plasticity are now classified under the rubric "short-term enhancement," defined as an activity dependent increase in synaptic efficacy produced by transient increases in residual presynaptic Ca^{2+} concentration (Fisher et al. 1997). Short-term enhancement has been separated into four distinct temporal phases (Zengel and Magleby 1982), F1, F2, augmentation (AUG), and posttetanic potentiation (PTP), lasting tens of milliseconds, hundreds of milliseconds, seconds, and tens of seconds, respectively. What we describe here in prefrontal cortex operates on the timescale of the latter two, AUG and PTP. For simplicity and because we have no mechanistic evidence demonstrating two separate processes in the prefrontal cortex, we refer to both phases collectively as "augmentation."

A large body of evidence links augmentation to increased residual presynaptic Ca^{2+} in model systems including the crustacean neuromuscular junction (Wojtowicz and Atwood 1988), vertebrate neuromuscular junction (Katz and Miledi 1968), and hippocampal CA3 (Regehr et al. 1994). Given this degree of phylogenetic conservation, it seems reasonable to hypothesize that the cortical augmentation described here would operate by the same mechanism. None of the data presented here are inconsistent with this hypothesis and two observations provide support. First, induction of augmentation at individual synapses demonstrates that it is a homosynaptic process not requiring widespread network activation or release of neuromodulators. Second, augmentation was observed under voltage-clamp conditions at −70 mV, ruling out mechanisms requiring strong postsynaptic depolarization.

Despite the similarities in augmentation between the prefrontal cortex and the model systems mentioned above, a number of differences exist. Most striking is the magnitude of the augmentation and the required amount of conditioning stimulation. Cortical augmentation saturated at ~40–60% enhancement after a moderate 15-stimulus, 50-Hz train (Fig. 4). By contrast, at the frog neuromuscular junction augmentation does not reach a limit even with 30-Hz trains of 30-s durations (Magleby and Zengel 1975). With such long trains, synaptic transmission can be increased up to fivefold, although this is under conditions of reduced Ca^{2+} and elevated Mg^{2+}. At mossy fiber synapses in the hippocampus, in the presence of physiological Ca^{2+} concentrations, extended conditioning trains (e.g., 3 s of 120 Hz) produce two- to threefold enhancement of synaptic transmission, whereas shorter trains produce less (Griffith 1990; Regehr et al. 1994). In both of these cases the dynamic range of synaptic enhancement and of the required conditioning stimulus were substantially larger than that observed in cortex, suggesting mechanistic differences. One pos-

sibility is that the expression of augmentation is limited by competing depression in the cortex. In sensorimotor cortex, an NMDA receptor dependent form of short-term enhancement has been observed (Castro-Alamancos and Connors 1996; Thomson et al. 1993). This raises the possibility of multiple mechanisms of short-term synaptic enhancement coexisting in the cortex.

The finding that augmentation was differentially expressed at prefrontal and visual cortical synapses suggests the possibility that the dynamic properties of synapses are specialized along different cortical pathways to allow expression of different patterns of activity. The differences we observed may reflect primarily an interareal difference or may reflect a difference between particular interlaminar pathways. We cannot answer this question here because our field-potential comparison was restricted to only one pathway in each area: the previously studied layer IV to II/III pathway in visual cortex (Varela et al. 1997) and the layer II/III to V pathway in prefrontal cortex. To assess whether these plasticity differences arise primarily within or between cortical areas it will be necessary to systematically and quantitatively examine plasticity properties in several pathways in each of the two cortical areas.

Possible functions of synaptic augmentation in the cerebral cortex

Although the functional role of augmentation has been difficult to assess at any of the wide variety of synaptic sites at which it is expressed, attempts have been made to link augmentation to various functions ranging from simple enhancement of neuromuscular transmission and temporal integration of neuronal signals to roles in learning and memory (reviewed by Fisher et al. 1997; Magleby 1987).

Here we present a specific hypothesis that may have particular relevance for cortical processing. We suggest that augmentation could act to enhance the ability of a neuronal circuit to sustain persistent activity evoked by a transient stimulus. In this scenario, augmentation would temporarily boost the level of recurrent excitation throughout a cortical network until it overcomes inhibitory transmission. This would lead to runaway excitation if not checked by short-term depression, which acts to limit the maximal total excitation in the network. We tested these ideas in a simple neuronal network model. Under the conditions tested, if the recurrent connections were not sufficiently strong, the model exhibited persistent activity in response to a transient input only when augmentation was present.

It has been generally assumed that persistent activity in the PFC is maintained by reverberation in a strongly recurrent network. Previous modeling studies have demonstrated that sufficiently strong recurrent connections can lead to network bistability between a resting state and a persistently active state (Amari 1977; Amit 1995; Camperi and Wang 1998; Wang 1999a). The results of this study suggest that synaptic augmentation may be a dynamic mechanism for temporarily boosting the efficacy of recurrent synapses. Such a mechanism offers several advantages compared with permanent synaptic enhancement (such as that induced by long-term potentiation). First, it may be more metabolically efficient to strengthen synapses temporarily during periods of persistent activity and

to conserve synaptic resources during periods of baseline activity. Second, temporary enhancement may provide greater flexibility and control. In this regard, it may be important that synaptic augmentation is activity dependent and can vary in a graded fashion depending on the level of neuronal firing. Finally, because the short-term plasticity of synapses can be strongly affected by manipulations that alter presynaptic release probability (Tsodyks and Markram 1997; Varela et al. 1997), an additional level of flexibility and regulation of persistent activity may be conferred by the action of neuromodulators such as dopamine. Further work will be required to determine whether dopamine and other neuromodulators have presynaptic actions at these synapses, and if so how these actions affect the dynamic properties studied here.

REFERENCES

ABBOTT, L. F., VARELA, J. A., SEN, K., AND NELSON, S. B. Synaptic depression and cortical gain control [see comments]. *Science* 275: 220–224, 1997.

AMARI, S. Dynamics of pattern formation in lateral-inhibition type neural fields. *Biol. Cybern.* 27: 77–87, 1977.

AMIT, D. J. The hebbian paradigm reintegrated: local reverberations as internal representation. *Behav. Brain Sci.* 18: 617–626, 1995.

ANGULO, M. C., STAIGER, J. F., ROSSIER, J., AND AUDINAT, E. Developmental synaptic changes increase the range of integrative capabilities of an identified excitatory neocortical connection. *J. Neurosci.* 19: 1566–1576, 1999.

BERTRAM, R., SHERMAN, A., AND STANLEY, E. F. Single-domain/bound calcium hypothesis of transmitter release and facilitation. *J. Neurophysiol.* 75: 1919–1931, 1996.

BUHL, E. H., TAMAS, G., SZILAGYI, T., STRICKER, C., PAULSEN, O., AND SOMOGYI, P. Effect, number and location of synapses made by single pyramidal cells onto aspiny interneurones of cat visual cortex. *J. Physiol. (Lond.)* 500: 689–713, 1997.

CAMPERI, M. AND WANG, X. J. A model of visuospatial working memory in prefrontal cortex: recurrent network and cellular bistability. *J. Comput. Neurosci.* 5: 383–405, 1998.

CASTRO-ALAMANCOS, M. A. AND CONNORS, B. W. Short-term synaptic enhancement and long-term potentiation in neocortex. *Proc. Natl. Acad. Sci. USA* 93: 1335–1339, 1996.

CHANCE, F. S., NELSON, S. B., AND ABBOTT, L. F. Synaptic depression and temporal response characteristics of V1 cells. *J. Neurosci.* 18: 4785–4799, 1998.

FENG, T. P. Studies on the neuromuscular junction. XXVI. The changes of the end-plate potential during and after prolonged stimulation. *Chin. J. Physiol.* 16: 341–372, 1941.

FISHER, S. A., FISCHER, T. M., AND CAREW, T. J. Multiple overlapping processes underlying short-term synaptic enhancement. *Trends Neurosci.* 20: 170–177, 1997.

FUNAHASHI, S., BRUCE, C. J., AND GOLDMAN-RAKIC, P. S. Mnemonic coding of visual space in the monkey's dorsolateral prefrontal cortex. *J. Neurophysiol.* 61: 331–349, 1989.

FUSTER, J. M. Unit activity in prefrontal cortex during delayed-response performance: neuronal correlates of transient memory. *J. Neurophysiol.* 36: 61–78, 1973.

GALARRETA, M. AND HESTRIN, S. Frequency-dependent synaptic depression and the balance of excitation and inhibition in the neocortex. *Nature Neurosci.* 1: 587–594, 1998.

GNADT, J. W. AND ANDERSEN, R. A. Memory related motor planning activity in posterior parietal cortex of macaque. *Exp. Brain Res.* 70: 216–220, 1988.

GRAFMAN, J., HOLYOAK, K. J., AND BOLLER, F. (EDITORS). *Structure and Functions of the Human Prefrontal Cortex.* New York: NY Acad. Sci., 1995.

GRIFFITH, W. H. Voltage-clamp analysis of posttetanic potentiation of the mossy fiber to CA3 synapse in hippocampus. *J. Neurophysiol.* 63: 491–501, 1990.

HIRSCH, J. C. AND CREPEL, F. Use-dependent changes in synaptic efficacy in rat prefrontal neurons in vitro. *J. Physiol. (Lond.)* 427: 31–49, 1990.

JAHR, C. E. AND STEVENS, C. F. Voltage dependence of NMDA-activated macroscopic conductances predicted by single-channel kinetics. *J. Neurosci.* 10: 3178–3182, 1990.

KATZ, B. AND MILEDI, R. The role of calcium in neuomuscular facilitation. *J. Physiol. (Lond.)* 195: 481–492, 1968.

KOLB, B. Prefrontal Cortex. In: *The Cerebral Cortex of the Rat*, edited by B. Kolb and R. C. Tees. Cambridge, MA: MIT Press, 1990, p. 437–458.

KUNO, M. Mechanism of facilitation and depression of the excitatory synaptic potential in spinal motoneurones. *J. Physiol. (Lond.)* 175: 100–112, 1964.

LLINÁS, R., STEINBERG, I. Z., AND WALTON, K. Relationship between presynaptic calcium current and postsynaptic potential in squid giant synapse. *Biophys. J.* 33: 323–351, 1981.

MAGLEBY, K. L. Short-term changes in synaptic efficacy. In: *Synaptic Function*, edited by G. M. Edelman, W. E. Gall, and W. M. Cowan. New York: Wiley, 1987, p. 21–56.

MAGLEBY, K. L. AND ZENGEL, J. E. A quantitative description of tetanic and post-tetanic potentiation of transmitter release at the frog neuromuscular junction. *J. Physiol. (Lond.)* 245: 183–208, 1975.

MALENKA, R. C. Postsynaptic factors control the duration of synaptic enhancement in area CA1 of the hippocampus. *Neuron* 6: 53–60, 1991.

MARKRAM, H., LUBKE, J., FROTSCHER, M., ROTH, A., AND SAKMANN, B. Physiology and anatomy of synaptic connections between thick tufted pyramidal neurones in the developing rat neocortex [In Process Citation]. *J. Physiol. (Lond.)* 500: 409–440, 1997.

MARKRAM, H. AND TSODYKS, M. Redistribution of synaptic efficacy between neocortical pyramidal neurons [see comments]. *Nature* 382: 807–810, 1996.

MARKRAM, H., WANG, Y., AND TSODYKS, M. Differential signaling via the same axon of neocortical pyramidal neurons. *Proc. Natl. Acad. Sci. USA* 95: 5323–5328, 1998.

MIYASHITA, Y. AND CHANG, H. S. Neuronal correlate of pictorial short-term memory in the primate temporal cortex. *Nature* 331: 68–70, 1988.

MORRIS, S. H., KNEVETT, S., LERNER, E. G., AND BINDMAN, L. J. Group I mGluR agonist DHPG facilitates the induction of LTP in rat prelimbic cortex. *J. Neurophysiol.* 82: 1927–1933, 1999.

NOWICKY, A. V. AND BINDMAN, L. J. The nitric oxide synthase inhibitor, *N*-monomethyl-L-arginine blocks induction of a long-term potentiation-like phenomenon in rat medial frontal cortical neurons in vitro. *J. Neurophysiol.* 70: 1255–1259, 1993.

PAXINOS, G. AND WATSON, C. *The rat brain in stereotaxic coordinates, 2nd ed.* San Diego, CA: Academic, 1986.

RAINER, G., ASAAD, W. F., AND MILLER, E. K. Memory fields of neurons in the primate prefrontal cortex. *Proc. Nat. Acad. Sci. USA* 95: 15008–15013, 1998.

REGEHR, W. G., DELANEY, K. R., AND TANK, D. W. The role of presynaptic calcium in short-term enhancement at the hippocampal mossy fiber synapse. *J. Neurosci.* 14: 523–537, 1994.

REYES, A., LUJAN, R., ROZOV, A., BURNASHEV, N., SOMOGYI, P., AND SAKMANN, B. Target-cell-specific facilitation and depression in neocortical circuits. *Nature Neurosci.* 1: 279–285, 1998.

ROMO, R., BRODY, C. D., HERNANDEZ, A., AND LEMUS, L. Neuronal correlates of parametric working memory in the prefrontal cortex. *Nature* 399: 470–474, 1999.

SCHOENBAUM, G. AND EICHENBAUM, H. Information coding in the rodent prefrontal cortex. I. Single-neuron activity in orbitofrontal cortex compared with that in pyriform cortex. *J. Neurophysiol.* 74: 733–750, 1995.

STEVENS, C. F. AND WANG, Y. Facilitation and depression at single central synapses. *Neuron* 14: 795–802, 1995.

TAMAS, G., SOMOGYI, P., AND BUHL, E. H. Differentially interconnected networks of GABAergic interneurons in the visual cortex of the cat. *J. Neurosci.* 18: 4255–4270, 1998.

TARCZY-HORNOCH, K., MARTIN, K. A., JACK, J. J., AND STRATFORD, K. J. Synaptic interactions between smooth and spiny neurones in layer 4 of cat visual cortex in vitro. *J. Physiol. (Lond.)* 508: 351–363, 1998.

THOMSON, A. M. Activity-dependent properties of synaptic transmission at two classes of connections made by rat neocortical pyramidal axons in vitro. *J. Physiol. (Lond.)* 502: 131–147, 1997.

THOMSON, A. M. AND DEUCHARS, J. Temporal and spatial properties of local circuits in neocortex. *Trends Neurosci.* 17: 119–126, 1994.

THOMSON, A. M., DEUCHARS, J., AND WEST, D. C. Large, deep layer pyramid-pyramid single axon EPSPs in slices of rat motor cortex display paired pulse and frequency-dependent depression, mediated presynaptically and self-facilitation, mediated postsynaptically. *J. Neurophysiol.* 70: 2354–2369, 1993.

THOMSON, A. M., WEST, D. C., HAHN, J., AND DEUCHARS, J. Single axon IPSPs elicited in pyramidal cells by three classes of interneurones in slices of rat neocortex. *J. Physiol. (Lond.)* 496: 81–102, 1996.

TSODYKS, M. V. AND MARKRAM, H. The neural code between neocortical pyramidal neurons depends on neurotransmitter release probability [published erratum appears in *Proc. Natl. Acad. Sci. USA* 94: 5495, 1997]. *Proc Natl Acad Sci U S A.* 94: 719–723, 1997.

UYLINGS, H.B.M., VAN EDEN, C. G., DE BRUIN, J.P.C., CORNER, M. A., AND FEENSTRA, M.G.P. (EDITORS). *The Prefrontal Cortex.* New York: Elsevier, 1990.

VARELA, J. A., SEN, K., GIBSON, J., FOST, J., ABBOTT, L. F., AND NELSON, S. B. A quantitative description of short-term plasticity at excitatory synapses in layer 2/3 of rat primary visual cortex. *J. Neurosci.* 17: 7926–7940, 1997.

VARELA, J. A., SONG, S., TURRIGIANO, G. G., AND NELSON, S. B. Differential depression at excitatory and inhibitory synapses in visual cortex. *J. Neurosci.* 19: 4293–4304, 1999.

WANG, X.-J. Synaptic basis of cortical persistent activity: the importance of NMDA receptors to working memory. *J. Neurosci.* 19: 9587–9603, 1999a.

WANG, X.-J. Fast burst firing and short-term synaptic plasticity: a model of neocortical chattering neurons. *Neuroscience* 89: 347–362, 1999b.

WOJTOWICZ, J. M. AND ATWOOD, H. L. Presynaptic long-term facilitation at the crayfish neuromuscular junction: voltage-dependent and ion-dependent phases. *J. Neurosci.* 8: 4667–4674, 1988.

ZENGEL, J. E. AND MAGLEBY, K. L. Augmentation and facilitation of transmitter release. A quantitative description at the frog neuromuscular junction. *J. Gen. Physiol.* 80: 583–611, 1982.

ZUCKER, R. S. Calcium and transmitter release. *J. Physiol. (Paris)* 87: 25–36, 1993.